

Anonymization for Skeleton Action Recognition

Myeonghyeon Kim
POSTECH

mhkim100@postech.ac.kr

Zhenyue Qin
Australian National University

zhenyue.qin@anu.edu.au

Yang Liu
Australian National University

yang.liu3@anu.edu.au

Dongwoo Kim
POSTECH

dongwookim@postech.ac.kr

Abstract

The skeleton-based action recognition attracts practitioners and researchers due to the lightweight, compact nature of datasets. Compared with RGB-video-based action recognition, skeleton-based action recognition is a safer way to protect the privacy of subjects while having competitive recognition performance. However, due to the improvements of skeleton estimation algorithms as well as motion- and depth-sensors, more details of motion characteristics can be preserved in the skeleton dataset, leading to a potential privacy leakage from the dataset. To investigate the potential privacy leakage from the skeleton datasets, we first train a classifier to categorize sensitive private information from a trajectory of joints. Experiments show the model trained to classify gender can predict with 88% accuracy and re-identify a person with 82% accuracy. We propose two variants of anonymization algorithms to protect the potential privacy leakage from the skeleton dataset. Experimental results show that the anonymized dataset can reduce the risk of privacy leakage while having marginal effects on the action recognition performance.

1. Introduction

Action recognition has been widely studied in many different applications such as sports analysis [23], human-robot interaction [4], and intelligent healthcare services [16]. Due to the success of convolutional neural networks, many recognition approaches are proposed based on a sequence of video frames. The action recognition can further be used for the public good. For example, with surveillance cameras in a public area or a school, we can detect violent actions.

To employ the recognition system appropriately, one must ensure that the private information is not abused after and before the analysis. Skeleton-based action recogni-

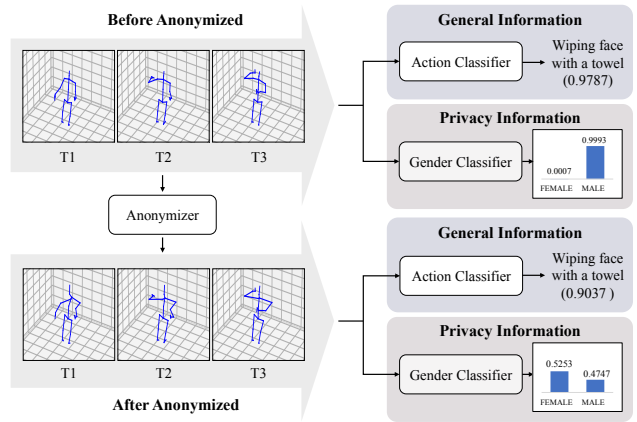


Figure 1. One example of privacy leakage from ETRI-activity3D datasets. A gender classifier is employed to identify the gender from a skeleton sequence, exposing the private gender information with high accuracy. After being anonymized, the action classifier is still capable of recognizing the action accurately while the privacy classifier hides the original gender information. Check the detailed experimental setup and results in [subsection 3.2](#).

tion can be an alternative to video-based recognition. Due to the advance of depth- and motion-sensors, details of motion characteristics can be preserved in the skeleton dataset. Compared with RGB-videos, a skeleton dataset seems to expose fewer details on participants. It is often challenging to identify sensitive information such as gender or age from a skeleton to compare with an RGB video to the naked eye.

We raise a question about the privacy-safeness of skeleton datasets. To check the potential privacy leakage from skeletons, we conduct experiments on identifying gender or identity with MSG3D action classification model [13]. As shown in [Figure 1](#), a properly trained classifier can predict the private information accurately. Therefore, the skeletons are not safe from the privacy leakage problem. A previous study [21] also confirms the possibility of identifying a per-

son from skeletons extracted from Kinect.

This work aims to develop a framework that can anonymize skeleton datasets while preserving critical action features for recognition. We propose a minimax framework to anonymize the skeletons with two learning algorithms. With RGB-video datasets, object detection followed by blurring or inpainting with pre-trained generative models is often employed to anonymize datasets [9, 26]. However, these methods cannot be directly applied to the skeleton dataset.

The minimax framework consists of an anonymizer network with two sub-networks designed to predict action and private information. The anonymizer removes private information from skeletons, and then the output skeleton is fed into action and privacy classifiers separately. We maximize the accuracy of the action classifier while minimizing the identifiability of private information with the other classifier. In addition, we enforce the anonymized skeleton similar to the original one to make sure they are visually indistinguishable from each other. A direct adversarial learning algorithm is proposed to solve the minimax problem. An ensemble-based learning algorithm is also proposed to solve the problem from a different perspective. The experimental results show that both algorithms result in an effective anonymizer.

We summarize our contributions as follows:

- We empirically show the potential privacy leakage from the widely-used skeleton datasets such as NTU60 [18] and ETRI-activity3D [10].
- We develop a skeleton anonymization network based on action and sensitive variable classifiers.
- We propose two learning algorithms to anonymize the skeletons: an ensemble method and an adversarial learning method.
- We show that the anonymized skeletons are more robust to privacy leakage while still enjoying high recognition accuracy.

2. Skeleton Anonymization

In this section, we propose a framework for the skeleton anonymization model. Then, two learning algorithms based on an ensemble method and an adversarial learning method are provided to learn the anonymization model.

Anonymization Framework. Let $\mathbf{x} \in \mathbb{R}^{T \times D \times 3}$ be 3D coordinates of D joints over T frames, and $y \in \mathcal{Y}$ be an action label for a given skeleton sequence \mathbf{x} , where \mathcal{Y} is a set of actions to be recognized. Let $z \in \mathcal{Z}$ be private information related to the skeleton sequence \mathbf{x} , e.g., a gender or an identity, where \mathcal{Z} is a set of possible private labels.

We aim to develop an anonymization network that can effectively remove private information from skeleton datasets while maintaining the recognizability of actions from the anonymized skeletons. To do this, we propose a minimax framework consisting of three different neural network components. Let $f_\theta : \mathbb{R}^{T \times D \times 3} \rightarrow \mathbb{R}^{T \times D \times 3}$ be an anonymizer network aiming to remove sensitive information from the input skeletons, $h_\psi : \mathbb{R}^{T \times D \times 3} \rightarrow \mathcal{Y}$ be an action classifier, and $g_\phi : \mathbb{R}^{T \times D \times 3} \rightarrow \mathcal{Z}$ be a privacy classifier that predicts sensitive personal information. Our goal is to train an anonymizer f_θ whose output can maximally confuse the classification performance on the private variables. On the other hand, the output of the anonymizer should keep all relevant information for recognizing action to preserve the performance of the action classifier h_ψ . In other words, the output should not be very different from the original skeletons since the anonymized skeletons can be recognizable by naked eyes. To satisfy all requirements, we formalize the anonymization via the following minimax objective:

$$\min_{\theta} \max_{\phi} \mathbb{E} \left[\text{CE}(y, h_\psi(f_\theta(\mathbf{x}))) - \alpha \text{CE}(z, g_\phi(f_\theta(\mathbf{x}))) + \beta \|\mathbf{x} - f_\theta(\mathbf{x})\|_2^2 \right], \quad (1)$$

where CE is the cross entropy, and α and β are hyper-parameters controlling the importance of the privacy classification and the reconstruction error, respectively. The reconstruction error between the original and anonymized skeleton data $\|\mathbf{x} - f_\theta(\mathbf{x})\|_2^2$ ensures the anonymized skeletons are similar to the original ones. To maximize the objective, the private classifier needs to classify the private label z correctly. To minimize the objective, the anonymizer makes the actions easily identifiable by action classifier h_ψ while making the private classifier misclassify the private label z . To simplify the learning process, we use a pre-trained action classifier and fix the parameters of the action classifier during training. The fixed action classifier constrains the anonymized skeleton compatible with the pre-trained model. The anonymized skeletons are also likely to work well with other pre-trained classifiers available.

Minimizing the objective w.r.t θ can make the anonymizer fool the private classifier. However, one may exploit this fact to infer the true label. For example, in a binary classification problem, the true label can be obtained by choosing the opposite of the prediction. To avoid this issue, we minimize the entropy of classified outputs during the minimization step:

$$\min_{\theta} \mathcal{L}_{\text{adv}} = \min_{\theta} \mathbb{E} \left[\text{CE}(y, h_\psi(f_\theta(\mathbf{x}))) - \alpha H(g_\phi(f_\theta(\mathbf{x}))) + \beta \|\mathbf{x} - f_\theta(\mathbf{x})\|_2^2 \right], \quad (2)$$

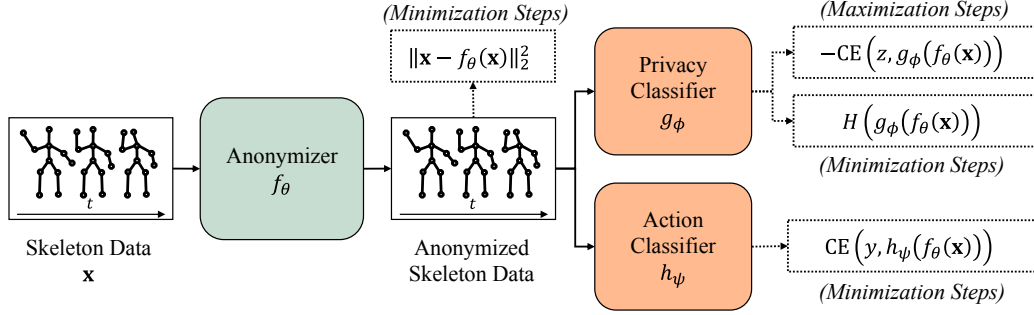


Figure 2. Anonymization framework. The framework consists of three sub-networks: 1) anonymizer f_θ , 2) privacy classifier g_ϕ , and 3) action classifier h_ψ . The dashed box represents the losses used in minimization and maximization steps with adversarial learning. Note that the privacy classifier uses a separate loss for minimization and maximization in adversarial learning setup. The parameter of the action classifier ψ is pre-trained and not updated during anonymizer training.

Algorithm 1 Adversarial Anonymization

Require: Pre-trained classifiers h_ψ and g_ϕ , E : # of epochs,
 m : minibatch size, k : # of minimization steps
while until convergence **do**
 for $t \leftarrow 1$ to k **do**
 Sample minibatch of m samples $\{(\mathbf{x}_i, y_i, z_i)\}_{i=1}^m$
 Compute $\nabla_\theta \mathcal{L}_{\text{adv}}$ with minibatch \triangleright Equation 2
 Update $\theta \leftarrow \theta - \nabla_\theta \mathcal{L}_{\text{adv}}$
 end for
 Sample minibatch of m samples $\{(\mathbf{x}_i, y_i, z_i)\}_{i=1}^m$
 Compute $\nabla_\phi \alpha \text{CE}(z, g_\phi(f_\theta(\mathbf{x})))$ with minibatch
 Update $\phi \leftarrow \phi - \nabla_\phi \alpha \text{CE}(z, g_\phi(f_\theta(\mathbf{x})))$
end while

where $H(g_\phi(f_\theta(\mathbf{x})))$ is the entropy of the distribution of private labels predicted from the anonymized skeleton. Therefore, the optimal anonymizer yields the most confusing skeletons to the private classifier. In the maximization step, we still maximize the negative cross entropy $-\alpha \text{CE}(z, g_\phi(f_\theta(\mathbf{x})))$ w.r.t. ϕ to train the private classifier. Figure 2 shows the overall framework for the data anonymization.

The minimax objective requires optimizing two sets of parameters θ, ϕ for the anonymizer and privacy classifier, respectively. We propose two different algorithms to optimize these parameters based on adversarial learning and ensemble learning.

Adversarial learning approach. Alternating minimization and maximization is often employed to solve a minimax objective as shown in the generative adversarial network [7]. Following previous work, we also use the alternating algorithm to optimize the objective. Algorithm 1 shows the overall training algorithm.

In this work, the adversarial learning algorithm starts

with pre-trained classifiers g_ϕ and h_ψ to make the learning stable. Empirically, we obtain a better anonymizer with the pre-trained models.

Ensemble-based approach. It is known that a minimax objective is difficult to optimize [17]. Here, instead of adversarial learning, we propose an ensemble-based learning algorithm to simplify the learning process. To avoid complex adversarial learning, we use pre-trained models to train an anonymizer. We first pre-train multiple action classifiers and privacy classifiers. With the pre-trained classifier, we directly optimize the following objective:

$$\min_{\theta} \mathcal{L}_{\text{ens}} = \min_{\theta} \mathbb{E} \left[\sum_{i=1}^N \text{CE}(y, h_{\psi}^{(i)}(f_{\theta}(\mathbf{x}))) - \alpha \sum_{i=1}^M H(g_{\phi}^{(i)}(f_{\theta}(\mathbf{x}))) + \beta \|\mathbf{x} - f_{\theta}(\mathbf{x})\|_2^2 \right], \quad (3)$$

where $h_{\psi}^{(i)}$ and $g_{\phi}^{(i)}$ are i th pre-trained classifiers, and N and M are the total number of pre-trained classifier for action and private information, respectively.

The anonymizer should output skeletons that work with multiple action classifiers and fool multiple privacy classifiers to minimize the objective. If the multiple classifiers learn different rules to classify, minimizing the objective results in a robust anonymizer that can work well with the classification models not used during the training. We empirically validate that increasing N and M can improve the anonymization performance. The overall training procedure of the ensemble method is shown in Algorithm 2.

Note that the ensemble learning approach can also be combined with the adversarial learning approach. However, the action and private classifiers in adversarial learning can adaptively change the prediction function based on the

changes in skeletons. Hence, the classifier with adversarial learning can potentially learn all possible prediction rules used in the ensemble method if the classifier is rich enough. To check the flexibility of adversarial learning, we use a single classifier in the experiments.

Anonymizer networks. The anonymizer f_θ can be any prediction model that modifies skeletons while preserving the original dimension. We employ two simple neural network architectures for the anonymizer: 1) residual networks and 2) auto-encoders.

The residual network [8] anonymizer adopts a simple residual connection from the input skeletons to the output skeletons. Specifically, the model can be formalized as

$$f_\theta(\mathbf{x}) = \text{MLP}_\theta(\mathbf{x}) + \mathbf{x},$$

where $\text{MLP}_\theta : \mathbb{R}^{D \times 3} \rightarrow \mathbb{R}^{D \times 3}$ is a simple multi-layered perceptron parameterized by θ . The residual connection keeps the position similar to the original skeleton while the MLP layer models the disposition of joints to anonymize. We use two fully-connected layers to model the disposition. The anonymizer is applied to each frame of a skeleton sequence. Although the anonymizer is applied to each frame independently, the back-propagated signals from action and private classifiers make the entire sequence coherent. By initializing θ with weights close to zero, we make the anonymizer add a small random noise to the original skeleton in the early stage of learning.

The auto-encoder anonymizer adopts a simple encoder-decoder architecture formalized as:

$$f_\theta(\mathbf{x}) = \text{Dec}(\text{Enc}(\mathbf{x})),$$

where $\text{Dec} : \mathbb{R}^{D \times 3} \rightarrow \mathbb{R}^H$ and $\text{Enc} : \mathbb{R}^H \rightarrow \mathbb{R}^{D \times 3}$ are the decoder and encoder parameterized by θ , where H is the size of the latent vector. In this work, we use two fully-connected layers for both encoder and decoder. To train the auto-encoder anonymizer, we pre-train the model by reconstructing the skeleton with a training dataset. The encoder layers are then fixed, and only the decoder layers are trained by Algorithm 1 or 2.

Note that the anonymizers used in this work employ relatively simple architectures. Experiments show that private information can be removed effectively even with the simple architecture.

3. Experiments

In this section, we demonstrate the performance of the proposed framework for anonymizing skeleton datasets. We use two publicly available datasets and anonymize two different types of private information: gender and identity.

Algorithm 2 Ensemble Anonymization

Require: Pre-trained classifiers $\{h_\psi^{(i)}\}_{i=1}^N$ and $\{g_\phi^{(i)}\}_{i=1}^M$
while until convergence **do**
 Sample minibatch of m samples $\{(\mathbf{x}_i, y_i, z_i)\}_{i=1}^m$
 Compute $\nabla_\theta \mathcal{L}_{\text{ens}}$ with minibatch ▷ Equation 3
 Update $\theta \leftarrow \theta - \nabla_\theta \mathcal{L}_{\text{ens}}$
end while

3.1. Datasets

We use two datasets: ETRI-activity3D [10] and NTU RGB+D 60 (NTU60) [18]. For the ETRI-activity3D dataset, we anonymize the gender information from the skeletons. For the NTU60 dataset, we anonymize the identity from the skeletons. The detailed experimental setups for these datasets are as follows.

ETRI-activity3D. ETRI-activity3D is an action recognition dataset originally published for recognizing the daily activities of the elderly and youths. It contains 112,620 skeleton sequence samples observed from 100 people, half of whom were between the ages 64 and 88 and the rest were in their 20s. The elderly consist of 23 females and 17 males, and the young adults consist of 25 females and 25 males. The samples are categorized into 55 classes based on the activity type. Each action is captured from 8 different Kinect v2 sensors to provide multiple views. Each sequence consists of 3D locations of 25 joints of the human body.

With the ETRI-activity3D dataset, we anonymize the gender information from the skeletons. We drop samples from 5 classes for the following experiments, *e.g.*, hand-shaking, containing two people, so only one person appears in the remaining samples. After removing malformed and two-person samples, we split the remaining samples into 68,788 and 34,025 training and validation, respectively. We split the dataset according to the subject ID. In other words, the subjects in the validation set do not appear in the training set. Through this split, we measure the generalizability of the gender classifier to the unknown subjects.

NTU60. NTU60 is an action recognition dataset that contains 60 action classes and 56,880 skeleton sequences taken from 40 subjects. The format of skeleton data is the same as ETRI-activity3D, which includes the 3D positions of 25 human body joints. After removing malformed samples, we split the remaining samples into 37,646 and 18,932 as training and validation sets, respectively. Following the original work [18], we split it according to the camera ID so that both sets contain identical subjects with different views.

	Accuracy	Agreement			
		G1	G2	G3	G4
G1	0.8805	1.00	0.89	0.90	0.89
G2	0.8767	0.89	1.00	0.91	0.91
G3	0.8801	0.90	0.91	1.00	0.91
G4	0.8788	0.89	0.91	0.91	1.00

Table 1. Gender classification accuracy of four classifiers and their pairwise agreement ratio on ETRI-activity 3D dataset. Four classification models, represented as G1 to G4, with different random seeds are trained. All models show similar accuracies.

	Accuracy		Agreement			
	Top-1	Top-5	A1	A2	A3	A4
A1	0.9219	0.9899	1.00	0.94	0.94	0.94
A2	0.9229	0.9909	0.94	1.00	0.93	0.93
A3	0.9209	0.9894	0.94	0.93	1.00	0.93
A4	0.9189	0.9893	0.94	0.93	0.93	1.00

Table 2. Top1 and top5 action classification accuracy of four MS-G3D classification models and their pairwise agreement ratio on ETRI-activity 3D dataset. Four models, represented as A1 to A4, are trained with different random seeds.

3.2. Privacy Leakage

To verify privacy leakage from each dataset, we first check the performance of gender classification and re-identification models. The gender classifier consists of MS-G3D [13] without a G3D module. This makes training much faster without losing too much accuracy. For the re-identification, we adopt the MS-G3D as a classification model. We train four classifiers for the gender classification task and two classifiers for the re-identification task. Each model is trained with a different random initialization.

Table 1 shows the results from the gender classification. As the results suggest, the gender information can be easily predicted by a classification model trained with the gender labels. Note that the test splits do not contain the subject used. This reveals the generalizability of gender classification to the unseen subjects. Due to the high accuracy, we find the classifiers also have a high agreement ratio, but still, there is disagreement between different classifiers.

For the re-identification task, the two classifiers achieve top-1 accuracy of 81.61% and 82.84% and top-5 accuracy of 97.46% and 97.56%, respectively. This result indicates that the joint trajectory contains personal traits that can be easily exploited to identify a person.

3.3. Anonymization Results

Based on the privacy leakage obtained in the previous experiments, we evaluate the performance of anonymization with two learning algorithms. We use the MS-G3D [13]

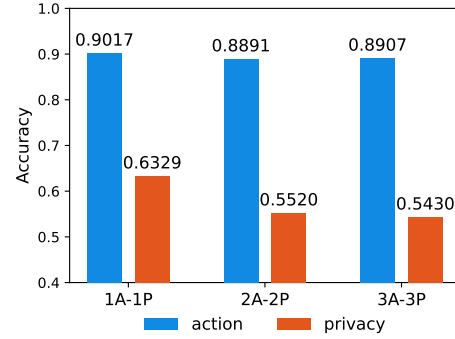


Figure 3. Classification accuracy vs the number of models used in an ensemble with the residual network anonymizer. $NA-NP$ indicates the use of N pre-trained action classifiers and N pre-trained privacy classifiers in the ensemble learning. The results are computed with the fourth classifier, which has not been used for training. As we increase the number of gender classifiers, the accuracy is getting close to random.

Model		Recon.	Action	Gender
Not-anonymized		0.0000	0.9189	0.8788
RN	$\sigma = 0.001$	0.0010	0.9141	0.8727
	$\sigma = 0.005$	0.0050	0.8790	0.8222
	$\sigma = 0.010$	0.0100	0.8445	0.6792
	$\sigma = 0.020$	0.0200	0.7800	0.6046
	$\sigma = 0.050$	0.0500	0.4980	0.6046
	$\sigma = 0.100$	0.1000	0.1162	0.6046
Ens.	Auto-encoder	0.0765	0.6664	0.5859
	ResNet	0.0271	0.8907	0.5430
Adv.	Auto-encoder	0.0839	0.5931	0.6102
	ResNet	0.0565	0.8425	0.5703

Table 3. Reconstruction error, action accuracy, and gender classification accuracy before and after anonymization. A root mean squared error is reported for the reconstruction error. We anonymize the skeletons using two different architectures. ‘Ens.’ denotes the ensemble with three models, and ‘Adv.’ denotes the adversarial learning. We report the results from the ensemble of three action and gender classifiers here. ‘RN’ shows the performances of skeletons with additional white noise drawn from $\mathcal{N}(0, \sigma^2)$ to each joint coordinate. 0.6046 is the proportion of the males in the dataset.

models for action classification.

Gender anonymization. To anonymize gender from the ETRI-activity3D dataset, we first train four action classifiers separately with different random seeds. These models are then used to optimize the ensemble and adversarial learning approaches with the four gender classifiers trained

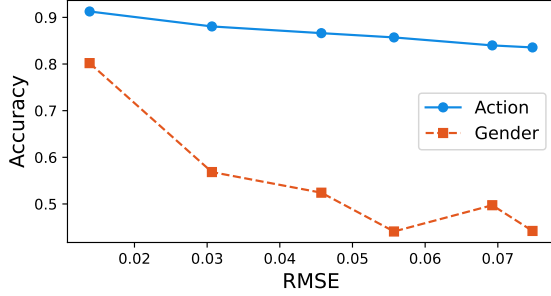


Figure 4. Reconstruction error vs. gender and action accuracy. We vary the hyperparameters to obtain different levels of the reconstruction error. As the reconstruction error increases, the action classification performance decreases.

in the previous section. We use MS-G3D as a baseline classifier for the actions. The classification performances on actions are reported in Table 2 with the pairwise agreement ratio between different classifiers.

To learn the anonymizer with an ensemble learning approach, we use the pre-trained models to minimize Equation 3. We increase the number of models that participate in the ensemble from one to three. The holdout model is then used to check the performance of the anonymized skeletons on the validation set. If the skeleton is anonymized well, the anonymized one should be compatible with the holdout action classifier while making the gender accuracy random. The detailed hyperparameter settings are available in the supplementary material. Figure 3 shows the gender and action classification accuracy of different ensemble sizes with the residual network based anonymizer. As we increase the number of both action and gender classifiers, the gender classification accuracy becomes random. A single classifier alone is not efficient enough to anonymize the skeletons in the ensemble.

To learn the anonymizer with an adversarial learning approach, we use the first pre-trained models to initialize Algorithm 1 and leave the fourth models to check the anonymization performance as done in the ensemble approach. In Table 3, we summarize the result with the ensemble and adversarial learning approaches. As a baseline, we randomly inject white noise drawn from the zero mean normal distributions to the original skeleton. Note that the random noise cannot preserve action information while reducing privacy leakage. The residual network based anonymizer performs better on both approaches than the auto-encoder based models. In general, we could not find a significant difference between the two approaches.

Reconstruction error analysis. A reconstruction error directly shows the level of difference between the original and anonymized skeletons. Although we cannot directly set the level of reconstruction error, we vary the parameters

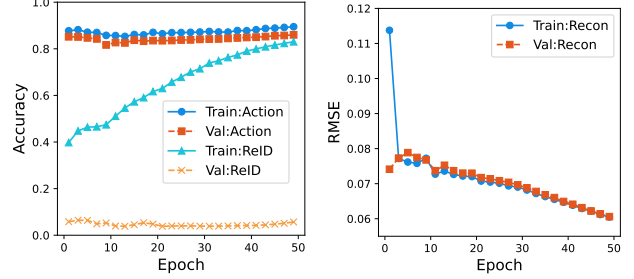


Figure 5. Accuracy and reconstruction error over epochs with the residual anonymizer in the adversarial learning method. ‘Train:Action’ and ‘Val:Action’ indicate the training and validation accuracy on the action classification, and ‘Train:ReID’ and ‘Val:ReID’ indicate the training and validation accuracy on the re-identification task. ‘Train:Recon’ and ‘Val:Recon’ indicate the root mean squared reconstruction errors. The action accuracy remains stable during training on both training and validation sets, whereas the re-identification accuracy drops at first and then increases over the epochs. The gap in validation and training accuracy for re-identification shows the classifier is overfitted to the training set.

to obtain different levels of reconstruction error and corresponding prediction accuracy. Please check the supplementary materials for the detailed hyper-parameter settings. As shown in Figure 4, there is a tradeoff between reconstruction error and gender accuracy. As we increase the reconstruction error, we can reduce the gender accuracy. However, high reconstruction error yields low action accuracy. Empirically, we find that the anonymized skeletons with reconstruction error around 0.05 give visually non-strange results while enjoying high action and low gender accuracy.

Identity anonymization. For the identity anonymization with NTU60, we use adversarial learning with the residual anonymizer since no significant difference is observed between the adversarial and ensemble learning from the previous experiment. We train two classifiers for action and identity, respectively. One classifier is used to initialize the adversarial algorithm, and the other is used to measure the accuracy after anonymization.

After anonymization, the holdout action classifier achieves an accuracy of 86.02%, and the re-identity classifier achieves an accuracy of 6.03%. We additionally plot how the validation accuracy changes over training procedure with adversarial learning in Figure 5. The action accuracy remains high over the epochs on both training and validation sets, whereas the re-identification accuracy drops first and then increases. However, the gap between the training and validation accuracy on identity shows the overfitting in the classifier. The validation accuracy at the first epoch indicates that the re-identification task is more sensitive to the additional noise introduced by random weights of the

residual network than the action classification.

Qualitative analysis. To qualitatively understand the effect of anonymization, we visualize three actions before and after anonymization in Figure 6. The top and bottom rows show five selected frames before and after anonymization for each figure, respectively. We can find some interesting patterns from the visualization. For example, in Figure 6a, the length of the neck bone is slightly increased, and the bone is moved to the upright position after anonymization. Given that an elderly female acts, we can conjecture that the adjustment makes gender unrecognizable.

4. Related work

Our work lies on the public data anonymization and skeleton-based action recognition. In this section, we provide the previous attempts on datasets anonymization and skeleton-based action recognition.

4.1. Public dataset anonymization

Researchers have pointed out privacy issues with public visual datasets and tried to mitigate them. [1], [6], and [26] propose a blurring approach where the privacy sensitive regions are blurred with an object detection method. [5] and [24] propose inpainting method to remove potentially problematic objects such as pedestrians and vehicles. While other works use traditional vision algorithms, [24] adopt a generative neural network model for the inpainting task and shown more realistic results. DeepPrivacy [9] also uses GANs [7] to generate fake faces to replace real ones. There also some works exist for other domains. For example, [3] blurs the voice of people recorded in a public space by using a U-Net based sound source separation model. Sümer *et al.* focus on anonymizing students voice in a classroom scenario [22]. In text domain, [12] and [2] propose a minimax problem to remove private information from text. Mosallanezhad *et al.* further advance the text anonymization with a reinforcement learning algorithm [15]. Malekzadeh *et al.* focus on data from mobile sensors such as accelerometer and gyroscope and show the potential leakage of private information therein [14]. The authors introduce an autoencoder-based anonymizer and adversarial optimization method.

Similar concerns are also made for skeleton datasets. Sinha *et al.* propose a method to recognize persons from skeleton data [21]. This work focuses on gait patterns extracted from human skeletons. The authors build a model with some predefined features and tested an adaptive neural network and naïve Bayes classifier for recognize identity of persons. This implies the potential privacy leakage from public datasets.

4.2. Skeleton-based action recognition

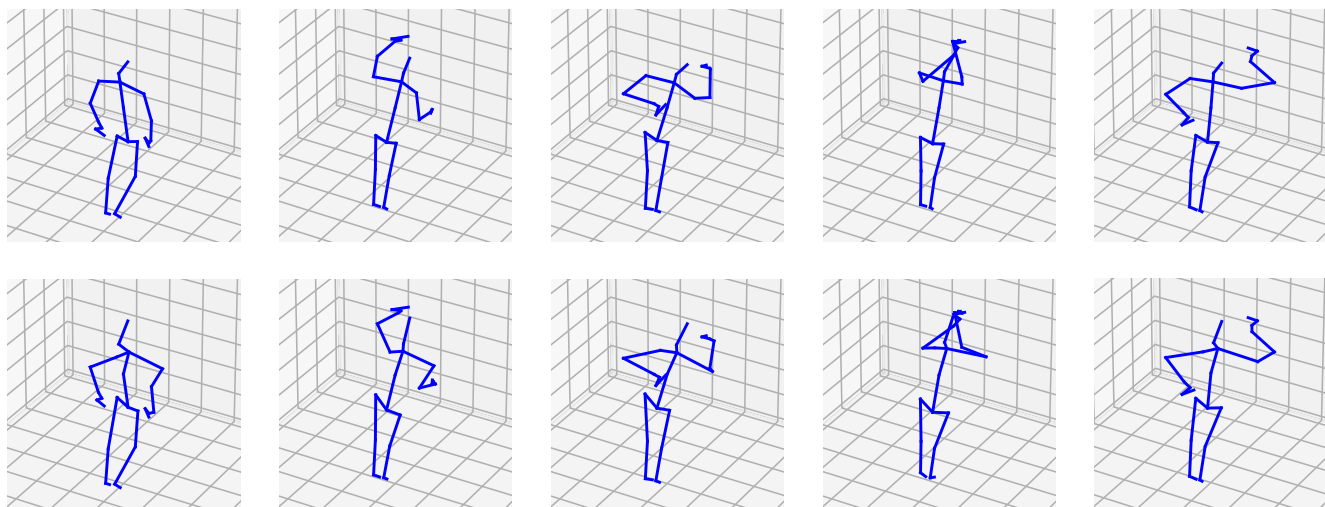
Human skeleton data is a sequence of graphs, where joints and bones are represented as nodes and edges separately within a graph. In early times, skeleton motion trajectories are embedded into a manifold space as points. The relative distances between these points acted as clues for action recognition. However, these models do not exploit the internal spatial relationship between joints. Later, convolution neural networks (CNNs) are utilized to extract spatial co-occurrence patterns between joints. Nevertheless, CNNs cannot model a skeleton’s topological information.

Then, graph convolution networks (GCNs) are introduced to model these topological relations. Nonetheless, basic GCNs are not suitable for human skeleton sequences because they contain not only the 3D position of joints but also the time series. Yan *et al.* introduces the spatial temporal graph convolutional networks (ST-GCN) [25]. They conduct graph convolution for extracting spatial features and perform 1×1 convolution over each joint for capturing temporal variations. Following this line, various graph neural architectures are proposed to extract features from the graphs. AS-GCN [11] applies parametric adjacency matrices to substitute for the fixed skeleton graph. Subsequently, AGC-LSTM [20] incorporates graph convolution layers into long short-term memory network (LSTM) as gate operations to capture long-range temporal movements in action sequences. The 2s-AGCN model [19] proposes bone features and learnable residual masks to enhance more flexibly extracting skeletons’ structural information and ensembles the models trained separately with joints and bones to improve the classification accuracy. MS-G3D [13] introduces cross-spacetime skip connections, which additionally connects all 1-hop neighbors across all time frames of a dilated sliding window for direct information flow, and shown improved recognition performance.

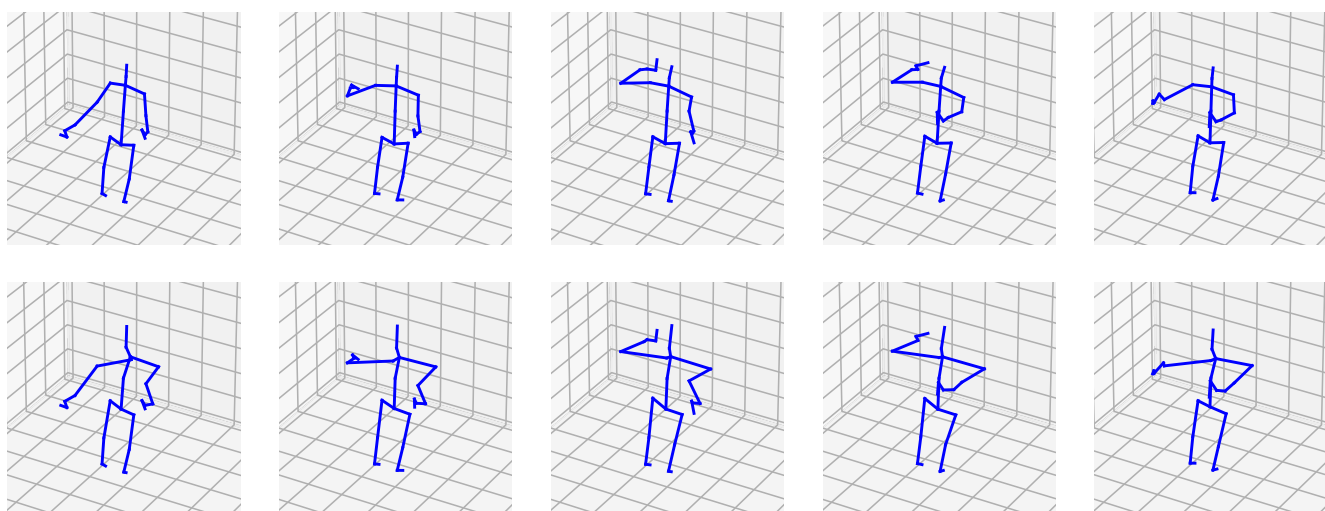
In this work, we use MS-G3D as a baseline recognition model for private information. Although the original model is developed to recognize the actions from skeletons, we empirically show the model can successfully classify the private information with a proper training procedure.

5. Conclusion

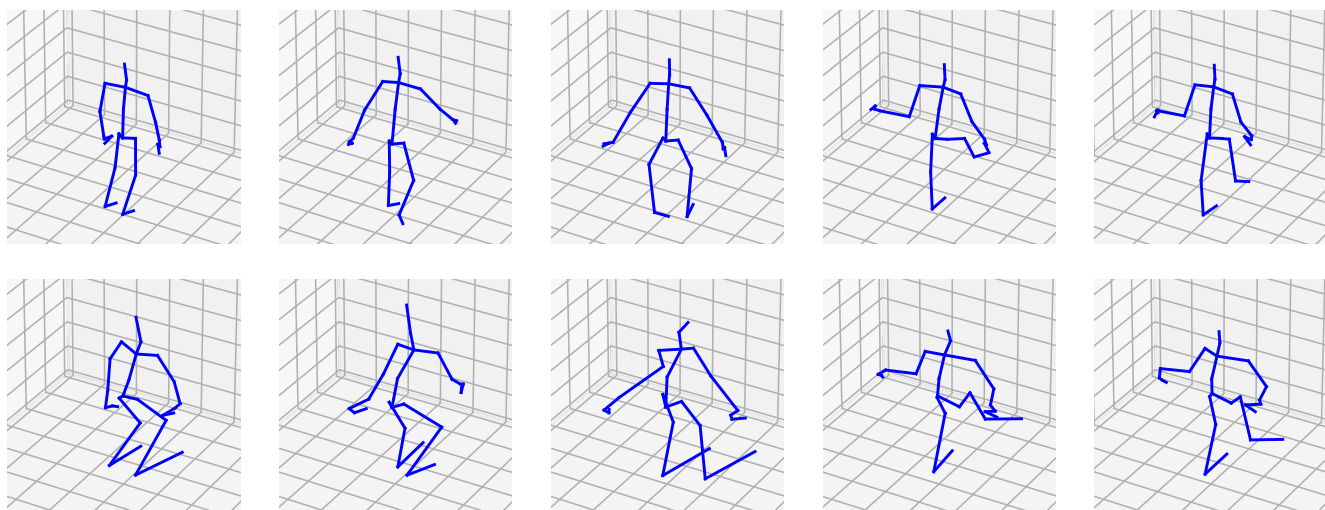
In this work, we investigate the privacy leakage from publicly available skeleton datasets. We show that although skeleton data may seemingly privacy protective, recently proposed skeletal action recognizers are surprisingly capable of extracting sensitive and identity information from these data. To address this privacy leakage problem, we propose a learning framework. Our experimental results reveal that the proposed method effectively remove the privacy information while preserves the movement patterns.



(a) The original (top) and the gender anonymized (bottom) skeletons for an action “wiping face with a towel” from ETRI-activity3D. The subject is an elderly female.



(b) The original (top) and the gender anonymized (bottom) skeletons for an action “drinking water” from ETRI-activity3D. The subject is an elderly male.



(c) The original (top) and the identity anonymized (bottom) skeletons for an action “kicking something” from NTU60. The subject’s ID is 2.

Figure 6. Examples of anonymized skeletons. Five frames are visualized from a sequence of action frames.

References

- [1] Holger Caesar, Varun Bankiti, Alex H Lang, Sourabh Vora, Venice Erin Liong, Qiang Xu, Anush Krishnan, Yu Pan, Giancarlo Baldan, and Oscar Beijbom. nuscenes: A multi-modal dataset for autonomous driving. In *Proceedings of the IEEE/CVF conference on computer vision and pattern recognition*, pages 11621–11631, 2020. 7
- [2] Maximin Coavoux, Shashi Narayan, and Shay B. Cohen. Privacy-preserving neural representations of text. In *Proceedings of the 2018 Conference on Empirical Methods in Natural Language Processing*, pages 1–10, Brussels, Belgium, Oct.-Nov. 2018. Association for Computational Linguistics. 7
- [3] Alice Cohen-Hadria, Mark Cartwright, Brian McFee, and Juan Pablo Bello. Voice anonymization in urban sound recordings. In *2019 IEEE 29th International Workshop on Machine Learning for Signal Processing (MLSP)*, pages 1–6. IEEE, 2019. 7
- [4] Sean Ryan Fanello, Ilaria Gori, Giorgio Metta, and Francesca Odone. Keep it simple and sparse: Real-time action recognition. *Journal of Machine Learning Research*, 14, 2013. 1
- [5] Arturo Flores and Serge Belongie. Removing pedestrians from google street view images. In *2010 IEEE Computer Society Conference on Computer Vision and Pattern Recognition-Workshops*, pages 53–58. IEEE, 2010. 7
- [6] Andrea Frome, German Cheung, Ahmad Abdulkader, Marco Zennaro, Bo Wu, Alessandro Bissacco, Hartwig Adam, Hartmut Neven, and Luc Vincent. Large-scale privacy protection in google street view. In *2009 IEEE 12th international conference on computer vision*, pages 2373–2380. IEEE, 2009. 7
- [7] Ian Goodfellow, Jean Pouget-Abadie, Mehdi Mirza, Bing Xu, David Warde-Farley, Sherjil Ozair, Aaron Courville, and Yoshua Bengio. Generative adversarial nets. *Advances in neural information processing systems*, 27, 2014. 3, 7
- [8] Kaiming He, Xiangyu Zhang, Shaoqing Ren, and Jian Sun. Deep residual learning for image recognition. In *Proceedings of the IEEE conference on computer vision and pattern recognition*, pages 770–778, 2016. 4
- [9] Håkon Hukkelås, Rudolf Mester, and Frank Lindseth. Deepprivacy: A generative adversarial network for face anonymization. In *International Symposium on Visual Computing*, pages 565–578. Springer, 2019. 2, 7
- [10] Jinhyeok Jang, Dohyung Kim, Cheonshu Park, Minsu Jang, Jaeyeon Lee, and Jaehong Kim. Etri-activity3d: A large-scale rgb-d dataset for robots to recognize daily activities of the elderly. In *2020 IEEE/RSJ International Conference on Intelligent Robots and Systems (IROS)*, pages 10990–10997. IEEE, 2020. 2, 4
- [11] Maosen Li, Siheng Chen, Xu Chen, Ya Zhang, Yanfeng Wang, and Qi Tian. Actional-structural graph convolutional networks for skeleton-based action recognition. In *Conference on Computer Vision and Pattern Recognition (CVPR)*, pages 3595–3603, 2019. 7
- [12] Yitong Li, Timothy Baldwin, and Trevor Cohn. Towards robust and privacy-preserving text representations. In *Proceedings of the 56th Annual Meeting of the Association for Computational Linguistics (Volume 2: Short Papers)*, pages 25–30, Melbourne, Australia, July 2018. Association for Computational Linguistics. 7
- [13] Ziyu Liu, Hongwen Zhang, Zhenghao Chen, Zhiyong Wang, and Wanli Ouyang. Disentangling and unifying graph convolutions for skeleton-based action recognition. In *Proceedings of the IEEE/CVF Conference on Computer Vision and Pattern Recognition (CVPR)*, June 2020. 1, 5, 7
- [14] Mohammad Malekzadeh, Richard G Clegg, Andrea Cavallaro, and Hamed Haddadi. Mobile sensor data anonymization. In *Proceedings of the international conference on internet of things design and implementation*, pages 49–58, 2019. 7
- [15] Ahmadrza Mosallanezhad, Ghazaleh Beigi, and Huan Liu. Deep reinforcement learning-based text anonymization against private-attribute inference. In *Proceedings of the 2019 Conference on Empirical Methods in Natural Language Processing and the 9th International Joint Conference on Natural Language Processing (EMNLP-IJCNLP)*, pages 2360–2369, 2019. 7
- [16] Alessia Saggese, Nicola Strisciuglio, Mario Vento, and Nicolai Petkov. Learning skeleton representations for human action recognition. *Pattern Recognition Letters*, 118:23–31, 2019. 1
- [17] Tim Salimans, Ian Goodfellow, Wojciech Zaremba, Vicki Cheung, Alec Radford, and Xi Chen. Improved techniques for training gans. *Advances in neural information processing systems*, 29:2234–2242, 2016. 3
- [18] Amir Shahrudy, Jun Liu, Tian-Tsong Ng, and Gang Wang. Ntu rgb+ d: A large scale dataset for 3d human activity analysis. In *Proceedings of the IEEE conference on computer vision and pattern recognition*, pages 1010–1019, 2016. 2, 4
- [19] Lei Shi, Yifan Zhang, Jian Cheng, and Hanqing Lu. Two-stream adaptive graph convolutional networks for skeleton-based action recognition. In *Proceedings of the IEEE/CVF conference on computer vision and pattern recognition*, pages 12026–12035, 2019. 7
- [20] Chenyang Si, Wentao Chen, Wei Wang, Liang Wang, and Tieniu Tan. An attention enhanced graph convolutional lstm network for skeleton-based action recognition. In *Proceedings of the IEEE/CVF Conference on Computer Vision and Pattern Recognition*, pages 1227–1236, 2019. 7
- [21] Aniruddha Sinha, Kingshuk Chakravarty, and Brojeshwar Bhowmick. Person identification using skeleton information from kinect. In *Proc. Intl. Conf. on Advances in Computer-Human Interactions*, pages 101–108, 2013. 1, 7
- [22] Ömer Sümer, Peter Gerjets, Ulrich Trautwein, and Enkelelda Kasneci. Automated anonymisation of visual and audio data in classroom studies. *arXiv preprint arXiv:2001.05080*, 2020. 7
- [23] Du Tran, Heng Wang, Lorenzo Torresani, Jamie Ray, Yann LeCun, and Manohar Paluri. A closer look at spatiotemporal convolutions for action recognition. In *Proceedings of the IEEE conference on Computer Vision and Pattern Recognition*, pages 6450–6459, 2018. 1
- [24] Ries Uittenbogaard, Clint Sebastian, Julien Vijverberg, Bas Boom, Dariu M Gavrila, et al. Privacy protection in street-

- view panoramas using depth and multi-view imagery. In *Proceedings of the IEEE/CVF Conference on Computer Vision and Pattern Recognition*, pages 10581–10590, 2019. [7](#)
- [25] Sijie Yan, Yuanjun Xiong, and Dahua Lin. Spatial temporal graph convolutional networks for skeleton-based action recognition. In *Thirty-second AAAI conference on artificial intelligence*, 2018. [7](#)
- [26] Kaiyu Yang, Jacqueline Yau, Li Fei-Fei, Jia Deng, and Olga Russakovsky. A study of face obfuscation in imagenet. *arXiv preprint arXiv:2103.06191*, 2021. [2](#), [7](#)

Appendix: Hyperparameter Configurations

Table 4 provides the detailed hyperparameter configurations used in the main results of the paper. Note that ‘etri’ indicates the ETRI-activity3D dataset and ‘ntu’ the NTU60 dataset. ‘ae’ is used to represent the auto-encoder based anonymizer, and ‘res’ the residual network based anonymizer. ‘lr min-step’ is the learning rate used for the minimization step. ‘lr max-step’ is used the learning rate used for the maximization step. Note that the ensemble approach does not have the maximization step. For all experiments, we use the SGD optimizer with momentum 0.9.

Table 5 provides the detailed hyperparameter configuration used to plot Figure 4 in the main paper.

	lr min-step	lr max-step	batch size	α	β
etri-ae-1a1p	0.00044	-	8	0.0045	0.0182
etri-ae-2a2p	0.00033	-	6	0.0045	0.0182
etri-ae-3a3p	0.00066	-	12	0.0045	0.0182
etri-ae-adv	0.00180	0.0030	24	0.1000	0.0067
etri-res-1a1p	0.00075	-	10	0.0333	0.0067
etri-res-2a2p	0.00060	-	8	0.0333	0.0067
etri-res-3a3p	0.00060	-	12	0.0333	0.0067
etri-res-adv	0.00180	0.0030	24	0.1000	0.0067
ntu-ae-adv	0.05000	0.0100	30	0.0400	0.1000
ntu-res-adv	0.00180	0.0030	24	0.1000	0.0067

Table 4. Hyperparameters used for the main experiments. We set $k = 1$ for adversarial anonymization, *i.e.*, one minimization with one maximization.

α	β	Recon. error (RMSE)	Action accuracy	Privacy accuracy
0.0067	0.0067	0.0138	0.9127	0.8019
0.0333	0.0333	0.0307	0.8806	0.5684
0.1000	0.0067	0.0457	0.8662	0.5242
0.1667	0.0067	0.0557	0.8570	0.4410
0.2333	0.0067	0.0692	0.8399	0.4973
0.3000	0.0067	0.0748	0.8356	0.4421

Table 5. Hyperparameters used to generate figure 4. For these experiments, we set the learning rate for the minimization step to 0.0018 and the maximization step 0.0030. For all experiments, we set $k = 2$, *i.e.*, two minimization with one maximization.